The *Plasmodium* translocon of exported proteins component EXP2 is critical for establishing a patent malaria infection in mice

Ming Kalanon,[1] Daniel Bargieri,[2,4] Angelika Sturm,[3] Kathryn Matthews,[1] Sreejoyee Ghosh,[1] Christopher D. Goodman,[3] Sabine Thiberge,[2] Vanessa Mollard,[3] Geoffrey I. McFadden,[3] Robert Ménard[2] and Tania F. de Koning-Ward[1]*

[1]*Molecular and Medical Research Unit, School of Medicine, Deakin University, Waurn Ponds, Geelong, Victoria 3216, Australia.*
[2]*Unité de Biologie et Génétique du Paludisme, Institut Pasteur, Paris, France.*
[3]*School of BioSciences, The University of Melbourne, Parkville, Victoria 3010, Australia.*
[4]*Department of Parasitology, Institute of Biomedical Sciences, University of São Paulo, São Paulo, SP Brazil.*

Summary

Export of most malaria proteins into the erythrocyte cytosol requires the *Plasmodium* translocon of exported proteins (PTEX) and a cleavable *Plasmodium* export element (PEXEL). In contrast, the contribution of PTEX in the liver stages and export of liver stage proteins is unknown. Here, using the FLP/FRT conditional mutatagenesis system, we generate transgenic *Plasmodium berghei* parasites deficient in EXP2, the putative pore-forming component of PTEX. Our data reveal that EXP2 is important for parasite growth in the liver and critical for parasite transition to the blood, with parasites impaired in their ability to generate a patent blood-stage infection. Surprisingly, whilst parasites expressing a functional PTEX machinery can efficiently export a PEXEL-bearing GFP reporter into the erythrocyte cytosol during a blood stage infection, this same reporter aggregates in large accumulations within the confines of the parasitophorous vacuole membrane during hepatocyte growth. Notably HSP101, the putative molecular motor of PTEX, could not be detected during the early liver stages of infection, which may explain why direct protein translocation of this soluble PEXEL-bearing reporter or indeed native

PEXEL proteins into the hepatocyte cytosol has not been observed. This suggests that PTEX function may not be conserved between the blood and liver stages of malaria infection.

Introduction

The pathology of malaria is linked to the ability of *Plasmodium* parasites to remodel their host erythrocyte during the intraerythrocytic development cycle (IDC) (Haase and de Koning-Ward, 2010; Boddey and Cowman, 2013). The remodelling process involves export of hundreds of parasite proteins beyond an encasing parasitophorous vacuole membrane (PVM) into the host cell, leading to consequential structural and biochemical changes to the erythrocyte. The majority of parasite proteins exported in the IDC contains a *Plasmodium* export element (PEXEL), consisting of a pentameric RxLxE/D/Q motif downstream of a signal peptide (reviewed in (Boddey and Cowman, 2013)), although some proteins lacking a PEXEL motif are also exported into the host cell. Both classes of exported proteins utilize the *Plasmodium* translocon of exported proteins (PTEX) (de Koning-Ward *et al.*, 2009) to translocate across the PVM and gain entry into the host erythrocyte (Beck *et al.*, 2014; Elsworth *et al.*, 2014).

Plasmodium translocon of exported proteins comprises of five known components (de Koning-Ward *et al.*, 2009). These include the AAA+ ATPase chaperone HSP101 that presumably unfolds protein cargo so that they are competent for export across the PVM, the putative pore-forming component EXP2, a thioredoxin protein TRX2, and two proteins named PTEX150 and PTEX88 of unknown function that are unique to malaria parasites. HSP101, PTEX150 and EXP2 are refractory to gene disruption (de Koning-Ward *et al.*, 2009; Matthews *et al.*, 2013; Matz *et al.*, 2013), indicating these core PTEX components are essential to the parasite's IDC, and knockdown of HSP101 and PTEX150 expression has validated that HSP101 and PTEX150 are indeed crucial for PTEX function and parasite growth in the IDC (Beck *et al.*, 2014; Elsworth *et al.*, 2014). Biochemical analysis of PTEX has revealed that these three core PTEX components associate as EXP2-PTEX150-HSP101, with EXP2 the component most tightly associated with the PVM

(de Koning-Ward *et al.*, 2009; Bullen *et al.*, 2012). Despite the lack of transmembrane domains, EXP2 is able to resist extraction from membrane fractions under high salt conditions and it remains in the carbonate insoluble fraction after carbonate extraction (Bullen *et al.*, 2012). Modelling of the predicted structure of EXP2 indicated similarity to HylE, an *Escherichia coli* α-pore forming toxin that forms dodecameric pores in host cell membranes (de Koning-Ward *et al.*, 2009). More recently, *Plasmodium falciparum* EXP2 has been shown to complement GRA17 function in *Toxoplasma* GRA17-deficient parasites (Gold *et al.*, 2015). Interestingly, similar to EXP2, GRA17 is also secreted from dense granules post-invasion, but this protein is predicted to play a role in nutrient access rather than protein export in *Toxoplasma gondii* (Gold *et al.*, 2015). Expression of EXP2 and GRA17 exogenously in *Xenopus* oocytes revealed that membrane conduction in the oocytes was altered in a manner consistent with EXP2 and GRA17 forming large non-selective pores (Gold *et al.*, 2015). Combined, the aforementioned studies are all in keeping with EXP2 forming the PVM-associated pore to which the rest of PTEX complex attaches, although whether the pore-forming capacity of EXP2 is restricted to PTEX function is unknown.

In addition to the asexual blood stages, several PTEX components are also transcribed or expressed at other parasite stages of the *Plasmodium* lifecycle, namely, sexual stage gametocytes, sporozoites and the liver stages (LS) of infection (Vaughan *et al.*, 2012; Matthews *et al.*, 2013). With respect to LS, the extent to which the parasite modifies its hepatic host cell is unknown. However, the vastly different cellular contexts between the erythrocyte and hepatocyte, including the presence of a nucleus, trafficking machinery and major histocompatibility complex Class I antigen presentation pathway, suggests that the process of host cell remodelling may be different between these two life cycle stages (Singh *et al.*, 2007; Cockburn *et al.*, 2011; Montagna *et al.*, 2014). In contrast to the hundreds of known exported proteins in the IDC, only two LS proteins have been shown to localize to the hepatic cytosol: circumsporozoite protein (CSP) (Singh *et al.*, 2007) and liver-stage specific protein 2 (LISP2) (Orito *et al.*, 2013). The role of PEXEL in mediating these LS protein translocations is unclear. An initial study using the N-terminus of CSP containing two PEXEL motifs to target GFP to the hepatic cytosol showed that mutating both motifs abrogated this localisation (Singh *et al.*, 2007). However, subsequent studies have shown that CSP with wildtype or mutated PEXEL localized to vesicular structures at the parasite periphery (Cockburn *et al.*, 2011) and that the N-terminus of CSP conjugated to ovalbumin (OVA) localized the reporter to the parasitophorous vacuole (PV) (Montagna *et al.*, 2014). PEXEL is also unlikely to contribute to LISP2 translocation, because the motif in this case is atypically located within the C-terminus of the protein and it is also not present in LISP2 orthologues in other

Plasmodium spp. (Orito *et al.*, 2013). Of note, no studies to date have demonstrated that proteins exported into erythrocyte cytosol during the IDC can also translocate into the hepatic host cell cytosol. Instead of translocation across the PVM, liver stage protein export from the parasite may be mediated by vesicular budding from the tubular-vesicular network (TVN) that extends from the PVM, as exemplified by IBIS1 and the CSP-PEXEL bearing OVA reporter (Ingmundson *et al.*, 2012; Montagna *et al.*, 2014).

In this study, we attempted to delineate the function of EXP2 during the IDC by regulating the expression of EXP2 in *P. berghei*. Failure of EXP2 expression to be adequately controlled using an anhydrotetracycline (ATc)-regulatable system led to the generation of a *P. berghei* conditional EXP2 knockout in the sporozoite stage of the life cycle, to explore the role of EXP2 and PTEX during the LS and transition to the IDC. The inclusion of a PEXEL-bearing reporter known to be exported in the IDC in the transgenic parasites also enabled investigations into whether soluble protein translocation into the hepatic cytosol occurs via a similar mechanism to the IDC. Our studies reveal that EXP2 is crucial for the ability of sporozoites to ultimately generate a patent infection in mice but unexpectedly that the PEXEL-bearing reporter was not translocated across the PVM in LS. This observation indicates that the role of PTEX may differ between the IDC and LS development.

Results

Creation of a Plasmodium berghei EXP2 conditional knockdown line using an anhydrotetracycline-regulatable system

As *P. berghei exp2* is refractory to gene deletion in the IDC (Matthews *et al.*, 2013; Matz *et al.*, 2013), studies on EXP2 necessitated the use of a gene regulatory system to explore its function in the PTEX complex and potentially additional roles for this protein in the IDC. For this, we used an approach successfully used to regulate the expression of *P. berghei* HSP101 to show that this protein is essential for protein export (Elsworth *et al.*, 2014). Herein, the transgenic line, PbiEXP2 KD was created, which harboured *exp2* under the transcriptional control of ATc-regulated transactivator elements (Fig. 1A). Transgenic parasites recovered after pyrimethamine selection and shown to contain the desired integration event by PCR (data not shown) were cloned by limiting dilution in mice and verified for clonality by Southern blot analysis (Fig. 1B). The growth of the PbiEXP2 KD parasites was then analysed in mice administered either ATc or vehicle control. Surprisingly, unlike the Pbi101 KD parasites, in which growth in mice was exquisitely sensitive to treatment with ATc, the parasitemias of PbiEXP2 KD parasites grown in the presence of ATc did not

A

B **C** **D**
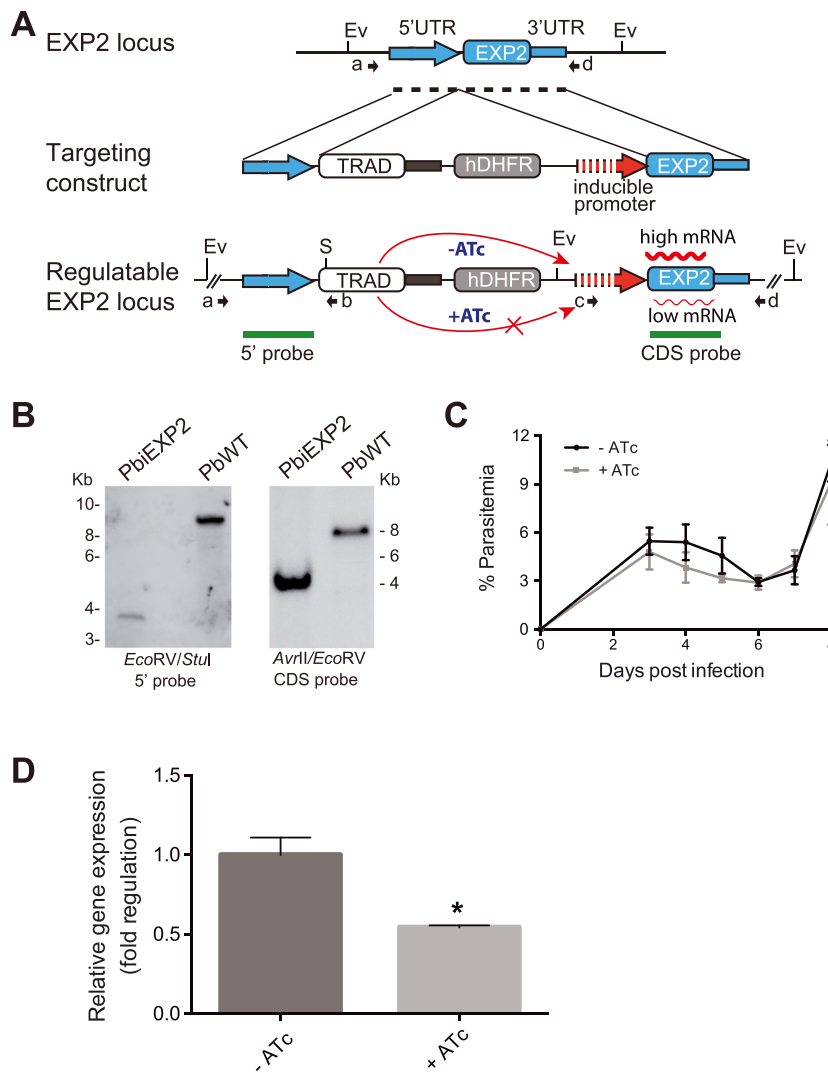
Fig. 1. A. Generation of an inducible knockout of *P. berghei* EXP2 (PbiEXP2 KD). The insertion of the targeting construct into the *exp2* locus results in incorporation of a TetR-AP2 transcriptional transactivator (TRAD) downstream of the *exp2* promoter. Transcription of *exp2* is under the control of an inducible minimal promoter and regulated by the addition of anhydrotetracyline (ATc). PCR primers used to detect 5′ integration (a/b; T56/T51), 3′ integration (c/d; T68/MK74) and wild-type locus (a/d; T56/MK74) are indicated. Ev, *Eco*RV; S, *Stu*I; A, *Avr*II.

B. Southern blot of genomic DNA from PbiEXP2 KD and PbANKA wild-type (WT) parasites using the 5′ UTR or CDS as a probe show the expected integrant band of 3.6 kb or 3.7 kb, respectively, in PbiEXP2 KD parasites and absence of bands corresponding to the WT locus.

C. Representative experiments ($n = 2$ independent experiments, five mice per group) performed in parallel shows PbiEXP2 KD *in vivo* growth is unaffected by ATc.

D. Quantitative RT-PCR on parasite material isolated from (C) shows approximately twofold knockdown of *exp2* transcript in PbiEXP2 KD parasites exposed to ATc.

significantly differ from parasites grown in the absence of ATc (Fig. 1C). Subsequent quantitative reverse transcriptase polymerase chain reaction (qRT-PCR) on schizonts stage parasites harvested from *in vitro* culture and grown in the presence or absence of ATc revealed that only modest knockdown of *exp2* transcription was achieved in ATc-treated parasites (Fig. 1D). Because EXP2 is a highly abundant protein in malaria parasites, and the conditional regulation of EXP2 in the IDC was not sufficient to influence growth and thus tease out potential phenotypes, we sought an alternative conditional regulation system to assess EXP2 function and to validate that EXP2 is indeed essential to malaria parasites.

Generation of Plasmodium berghei EXP2 conditional knockdown lines using the FLP/FRT recombinase system.

As the ATc-regulatable system is currently the only conditional system available to regulate EXP2 expression in the IDC stages of *P. berghei*, we turned to using the FLP recombinase in combination with FRT site-specific recombination sequences to delete a region of the *exp2* locus in sporozoites to assess the consequences on parasite infectivity and protein export in the LS (Combe *et al.*, 2009; Lacroix *et al.*, 2011). For this, the targeting constructs pEXP2-FRT or pEXP2-2A-FRT were designed such that upon integration into the *exp2* locus, the EXP2 3′ untranslated region (UTR) would be replaced with the thrombospondin related anonymous protein (TRAP) 3′ UTR and a selectable marker flanked by FRT-recombination sequences (Fig. 2A and B). The pEXP2-2A-FRT integration construct differs from pEXP2-FRT in that the sequence encoding the EXP2 CDS is fused to the foot and mouth disease virus 2a peptide (2A) and mCherry, used as a reporter of EXP2 expression. Upon integration, the placement of the 2A peptide results in the production of a polycistronic mRNA transcript that results in separate polypeptides, with EXP2 tagged by 2A but not
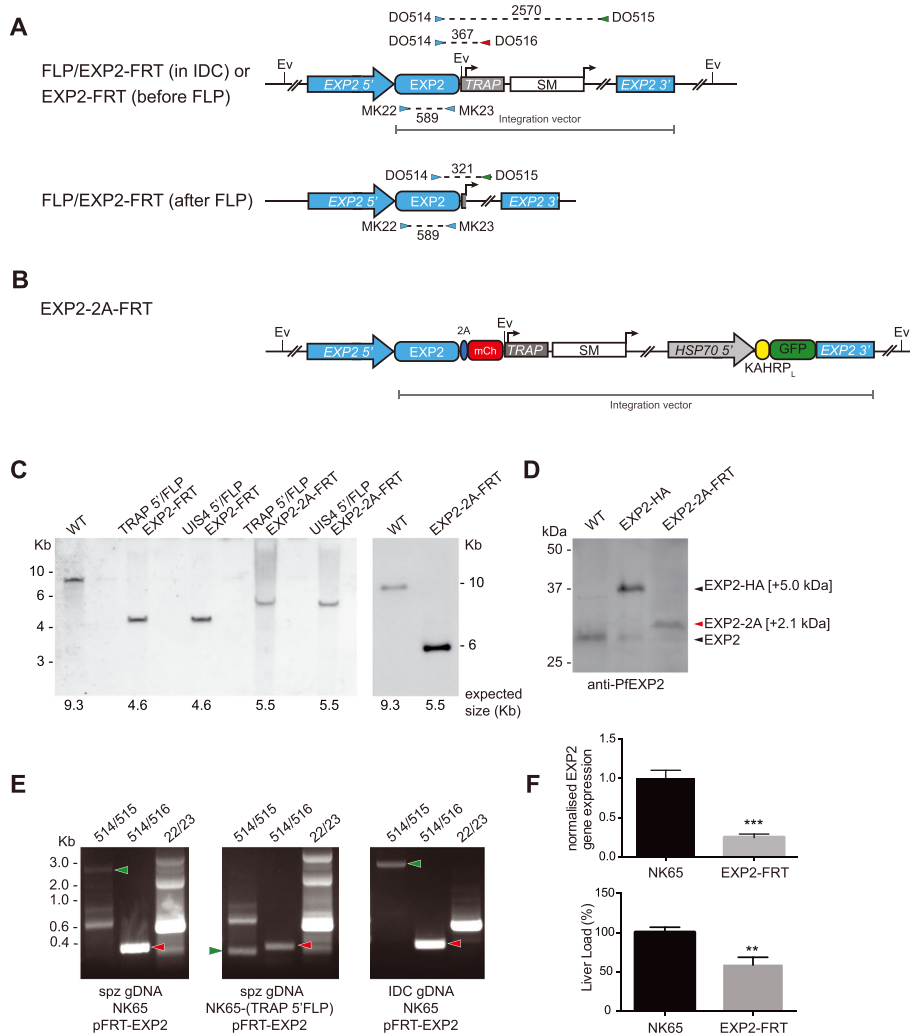
Fig. 2. A. Schematic of the *exp2* locus in FLP/EXP2-FRT parasites in the intraerythrocytic developmental cycle (IDC) before excision or after excision in the sporozoites. FRT recognition sequences are depicted by arrows, a grey line highlights the integration vector and expected sizes of the PCRs are indicated by dashed lines. SM, selectable marker. The oligonucleotide combinations DO380/DO381, DO381/DO221 and MK22/MK23 were used to verify that correct integration had occurred.
B. Schematic of the *exp2* locus in transgenic parasites that had been modified to incorporate a reporter of EXP2 expression, 2A-mCherry (mCh), and a reporter of translocation, KAHRP$_L$-GFP, the latter of which is placed under the transcriptional control of the HSP70 promoter (HSP70 5′).
C. Southern blot of genomic DNA isolated from wild-type (WT) or transgenic parasite lines digested with *Eco*RV and hydrized with the EXP2 CDS as a probe. The increase in the molecular weight of the hybridized band in TRAP 5′/FLP EXP2-2A-FRT and UIS 5′/FLP EXP2-2A-FRT when compared with TRAP 5′/FLP EXP2-FRT corresponds to the incorporation of the 2A-mCh coding sequence.
D. Western blot of saponin-lysed IDC parasites probed with anti-PfEXP2 antiserum reveals that EXP2-2A-mCh is effectively cleaved in PbTRAP-FLP/EXP2-2A-FRT parasites.
E. Representative PCR of genomic DNA derived from sporozoites (left and middle panel) or IDC with the primers as indicated reveal excision of the *exp2* locus has occurred only in parasites expressing the FLP recombinase ($n = 2$).
F. *Exp2* transcript in the livers of mice inoculated intravenously with PbTRAP-FLP/EXP2-FRT and PbEXP2-FRT (no FLP control) sporozoites at 48 h post-infection measured by qRT-PCR and normalized to parasite 18S ribosomal RNA (upper panel) and liver load quantification measured by qRT-PCR of parasite 18S ribosomal RNA normalized to *hprt* (upper panel) ($n = 6$). *** $P < 0.001$; ** $P < 0.01$.

with mCherry (Straimer *et al.*, 2012). Additionally, pEXP2-2A-FRT harbours an exported reporter cassette in which the N-terminal leader of the knob-associated histidine rich protein (KAHRP$_L$) has been conjugated to GFP (Fig. 2B) and is under the transcriptional control of the strong constitutive promoter of *HSP70*.

Both pEXP2-FRT or pEXP2-2A-FRT were transfected independently into either *P. berghei* NK65 wildtype parasites or *P. berghei* NK65-TRAP 5'/FLP or NK65-UIS 5'/FLP parasites. The latter two parasite lines express the FLP recombinase under the TRAP or upregulated in sporozoites (UIS) promoter, respectively, and hence should facilitate

excision of the TRAP 3' UTR and selectable marker through the recognition of the FRT sequences when parasites reach the sporozoite stages in the mosquito. Following transfection, parasites resistant to pyrimethamine selection were PCR genotyped (data not shown) and verification that correct integration had occurred was confirmed by Southern blot analysis using the EXP2 coding sequence (CDS) as a probe (Fig. 2C). For parasites transfected with pEXP2-2A-FRT, we additionally confirmed integration of the 2A-mCherry and KAHRP$_L$-GFP reporters by Western blotting of saponin-lysed IDC-stage parasites using the cross-reactive anti-PfEXP2 antibody (Fig. 2D). For controls, wildtype parasites and previously characterized *P. berghei* EXP2-HA parasites expressing EXP2 fused to three haemagluttinin epitopes and a streptavidin tag were used in the analysis (Matthews *et al.*, 2013). Consistent with previous results, the anti-PfEXP2 antiserum detected *P. berghei* EXP2 at approximately 26 kDa in wildtype parasites and EXP2-HA at approximately 32 kDa (Fig. 2D, black arrows), whereas in the EXP2-2A-FRT saponin lysate, a 28 kDa protein corresponding to the expected mass of EXP2-2A after cleavage of mCherry was detected (Fig. 2D, red arrow). As expected, an unprocessed EXP2-2A-mCherry protein was not detected at the predicted mass of 56 kDa.

As the aforementioned analyses confirmed that the desired integrants had been obtained and that the parasite lines were clonal, *Anopheles stephensi* mosquitoes were then allowed to feed on mice infected with the wildtype and FLP/FRT parasite lines. All parasite lines were capable of establishing an infection in mosquitoes and on day 23 post-transmission, after the mosquitos had been shifted to a temperature of 26°C for 7 days, salivary gland sporozoites were recovered. Analysis of the *exp2* locus was performed using oligonucleotides combinations in PCRs that would discriminate between excised and non-excised loci (Fig. 2A). Figure 2E shows a representative gel of PCRs performed on genomic DNA (gDNA) isolated from IDC PbFLP/EXP2-FRT, sporozoite Pb wildtype or sporozoite PbFLP/EXP2-FRT parasites. This revealed that gDNA from all samples amplified a 589 bp fragment as expected with oligonucleotides MK22/MK23 corresponding to the EXP2 CDS. In contrast, only a 321 bp fragment corresponding to the size of the excised 3' UTR could be amplified using oligonucleotides DO514/DO515 from the PbFLP/EXP2-FRT line, consistent with this line being the only one expressing the recombinase (Fig. 2E). Although a 2.75 Kb band corresponding to an intact *exp2* locus could not be detected in PbFLP/EXP2-FRT using DO514/DO515, the oligonucleotide combination DO514/DO516 generated a weak 367 bp product, indicating the presence of some non-excised parasites in this line (Fig. 2E). The inability of the FLP recombinase to excise at 100% efficiency is consistent with previous reports (Combe *et al.*, 2009; Giovannini

et al., 2011; Lacroix *et al.*, 2011; Zhang *et al.*, 2012; Tawk *et al.*, 2013). The 367 bp product representing non-excised DNA could be readily amplified from gDNA extracted from IDC PbFLP/EXP2-FRT and sporozoite Pb/EXP2-FRT, which is expected given that the recombinase is either not yet active or absent in these lines respectively (Fig. 2E).

EXP2 plays a crucial role in establishing a patent infection in mice

The FLP/FRT transgenic lines derived in this study were next examined for their ability to establish a patent infection in mice. Accordingly, 5000 sporozoites from each transgenic line were intravenously inoculated into mice and examined for when a blood parasitemia was first detectable. Nine out of the 10 mice inoculated with parasites either lacking the FLP recombinase or the FRT sites in the *exp2* locus (i.e. control parasites) developed a patent infection by either day 5 or 6 post-inoculation (Table 1). In contrast, 8 out of 13 mice inoculated with parasites containing both an FLP recombinase in conjunction with FRT sites in the *exp2* locus did not become infected by day 14 post-infection. Of the 5 out of 13 mice that did become infected, all but one of these mice exhibited a significant delay in patency of between 4 and 6 days. Similar patency results were achieved regardless of whether the mCherry and knob-associated histidine-rich protein conjugated to GFP (KAHRP$_L$-GFP) reporters were integrated into the *exp2* locus. This demonstrates a crucial role for EXP2 in parasite infectivity. These results are in keeping with an essential role for EXP2 in the PTEX complex in the IDC and the requirement for EXP2 to be at least expressed in the late LS to facilitate the establishment of the PTEX complex as soon as the LS merozoites are released into the blood stream and invade erythrocytes. Indeed, EXP2 has been shown to be expressed in LS merozoites (Matthews *et al.*, 2013). However, EXP2 may also be required during the pre-erythrocytic phase of parasite development. To assess this, qRT-PCR was performed on RNA isolated from livers extracted from

Table 1. EXP2 is required to establish a patent infection in mice.

Parasite line	No. of positive mice/ no. of injected mice	Time to patency (days)*
Without reporter cassette		
Control: PbTRAP FLP	3/3	6
Control: PbEXP-FRT	3/4	5
PbTRAP FLP/EXP2-FRT	2/7	6, 10 *
PbUIS4 FLP/EXP2-FRT	0/3	N/A*
With mCherry and KAHRP$_L$-GFP reporter cassette		
Control: PbEXP-2A-FRT	3/3	6
PbTRAP FLP/EXP2-2A-FRT	3/3	10, 10, 12*

*Significant difference in patency compared with control lines: log-rank (Mantel-Cox) test, $P < 0.05$.

mice inoculated intravenously with salivary gland sporo-zoites at 48 hrs post-infection. The abundance of *exp2* transcript synthesized at this time was significantly lower in the NK65-(TRAP 5′ FLP)/EXP2-FRT parasites when compared with NK65/EXP2-FRT parasites (Fig. 2F, upper panel), which is consistent with the results in Fig. 2E showing the *exp2* locus is excised in sporozoites, albeit not at 100% efficiency. Additionally, when the abundance of *P. berghei* 18S rRNA was measured relative to mouse hypoxanthine guanine phosphoribosyltransferase (*hprt*), this revealed that although NK65-(TRAP 5′ FLP)/EXP2-FRT parasites were present in the liver, the liver load was significantly lower than that of NK65/EXP2-FRT parasites (Fig. 2F, lower panel).

*Analysis of protein export in liver stages*

One way to further confirm whether EXP2 plays a potential role in the LS was to examine protein export in the conditional knockdown lines FLP/EXP2-2A-FRT before and after excision by live epifluorescent imaging. Because a robust LS exported reporter has yet to be identified, the soluble exported protein KAHRP$_L$-GFP reporter was used in these studies because the sequences facilitating export of KAHRP are known, and this reporter has been shown to be efficiently translocated into the erythrocyte cytosol of *P. berghei* (Haase *et al.*, 2013). The HSP70 promoter driving expression of this reporter has also been shown to be a strong and constitutive promoter throughout the *P. berghei* lifecycle (Hliscs *et al.*, 2013) and thus overex-pression of the reporter maximizes the chances of detecting fluorescence in the hepatocyte cytosol (Haase *et al.*, 2009; Sijwali and Rosenthal, 2010).

Firstly, the localisation of mCherry and KAHRP$_L$-GFP in FLP/EXP2-2A-FRT parasites was examined in the IDC (Fig. 3A). As expected, the KAHRP$_L$-GFP reporter was detected in the erythrocyte cytosol as well as in a reticular structure in the parasite that is consistent with the parasite secretory system. A detectable signal was also observed at the PVM and TVN (Fig. 3A, white arrows). The mCherry reporter was localized to the parasite cytosol (Fig. 3A), consistent with its independent translation from EXP2 and its lack of any trafficking motif.

Surprisingly, however, KAHRP$_L$-GFP did not localize to the hepatocyte cytosol in unfixed hepatocytes infected with non-excised EXP2-2A-FRT parasites (Fig. 3B and C). Instead, at 20 h post-infection (hpi), GFP delineated the characteristically round early exo-erythrocytic form of the parasite (Fig. 3B), consistent with PV labelling (Ingmundson *et al.*, 2012; Grutzke *et al.*, 2014). At this stage of LS development, weak mCherry expression was detected in the parasite cytosol, indicating low levels of EXP2 expression. Even when the level of mCherry expression increased significantly during mid LS infection, indicating more abundant levels of EXP2 expression (44 hpi; Fig. 3B, middle panel, and C), KAHRP$_L$-GFP had still

not translocated into the hepatocyte cytosol. By the time the merosome had formed (62 hpi; Fig. 3B, bottom panel), the KAHRP$_L$-GFP signal surrounding the mCherry puncta was diffuse, but held within the spherical merosome sac. This localisation is consistent with the disruption of the PVM upon merosome formation (Sturm *et al.*, 2006; Sturm *et al.*, 2009). We could confirm that KAHRP$_L$-GFP was bounded by the PVM, as 20 hpi EXP2-2A-FRT parasites fixed under hypotonic conditions and labelled with anti-PbEXP1 antibody (a PVM marker) showed GFP co-localized predominantly with EXP1, with a significant average Pearson's coefficient value of 0.716 (Fig. 3D, upper panel). However, under these hypotonic fixation conditions, the large peripheral bulges seen at 48 hpi by live cell imaging were disrupted, and KAHRP$_L$-GFP was distributed throughout the hepatic cytosol indicating that the lack of KAHRP$_L$-GFP detection in the hepatic cytosol in unfixed parasites at 48 hpi did not appear to be due to a failure of fluorescence detection *per se* (Fig. 3D, lower panel). It is likely that the PVM was not disrupted in a similar way at 20 hpi because these earlier parasites lacked the large bulges that had accumulated by 48 hpi.

The inability to detect exported KAHRP$_L$-GFP in non-excised EXP2-2A-FRT parasites therefore precluded the possibility of comparing the degree of export of KAHRP$_L$-GFP in EXP2-2A-FRT parasites that had undergone excision to those parasites that had not. Although the accumulation of GFP in large, discrete bulges within the confines of the PVM, clearly visible in the transmission images of the parasite, but not inside the parasite cytosol (Figs. 3B and C) most likely stems from the over-expression of the GFP, the expansion of the PV space nevertheless provided a unique opportunity to examine its organisation. The images revealed that there are distinct regions of close proximity between the PVM and the parasite plasma membrane in LS (for example, Fig. 3B, yellow arrows). This indicates there is a tight association between these two membranes at junctions around the parasite, reminiscent of the 'necklace of beads' PV morphology observed in the IDC (Wickham *et al.*, 2001; Tilley *et al.*, 2007). Interestingly, in parasites at the 18–24 h stage, protrusions of KAHRP$_L$-GFP were also evident in the majority of parasites (Figs. S1 and 4) and are similar to the extended membrane clusters and tubules described by Grutzke and colleagues (Grutzke *et al.*, 2014). Extended membrane clusters were observed in 100% of parasites, whilst tubules were observed in 40% (*n* = 27). Of these, 80% displayed protrusions (clusters or tubules) that orientate towards the host nucleus. In some cases, the orientation towards the host nucleus correlated with indentations or grooves in the host nucleus (Fig. 4, white arrows). Whether these close associations are physiolog-ically relevant (for example, represent communication with the host cell) will nevertheless require further analysis.
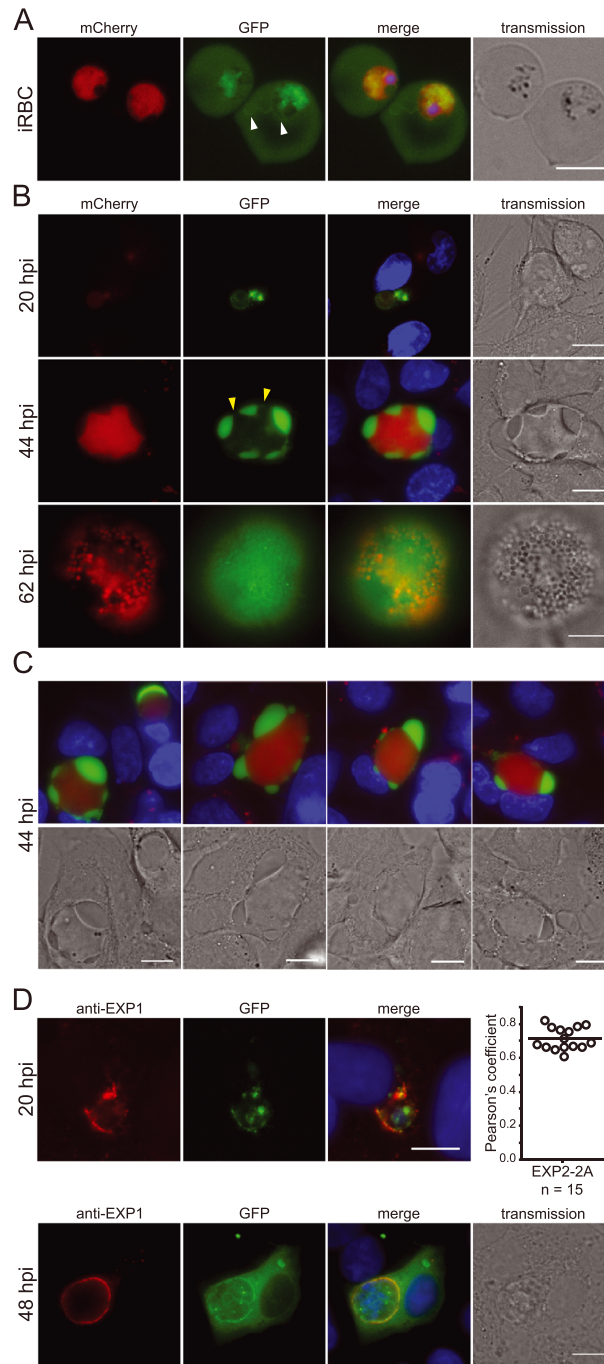
Fig. 3. A. Epifluorescent imaging of unfixed IDC PbTRAP-FLP/EXP2-2A-FRT parasites (which contain the KAHRP$_L$-GFP expression cassette) shows that mCherry (mCh) localizes to the parasite cytosol and KAHRP$_L$-GFP is translocated to the erythrocyte cytosol. GFP can also be detected in the TVN and PV of the infected erythrocyte (white arrows). Scale bars 5 μm.

B. Epifluorescent imaging of unfixed non-excised PbTRAP-FLP/EXP2-2A-FRT infected hepatocytes shows that KAHRP$_L$-GFP is held in the PV of 20 hpi LS infection, where mCh is expressed at very low levels. KAHRP$_L$-GFP accumulates in the PV of mid LS parasites (44 hpi), forming large bulges clearly visible in the transmission field. Points of close apposition between the PVM and PM are also clearly observed (yellow arrows). At this stage, mCh is clearly detectable, indicating new EXP2 translation. Late LS parasites (62 hpi) have formed merosomes with individual merozoites expressing mCh, and KAHRP$_L$-GFP localizes within the merosome sac. Scale bars 10 μm.

C. Further examples of the large accumulations of GFP at the parasite periphery at 44 hpi, which can clearly be seen in the transmission image. Scale bars 10 μm. D. Fixation of non-excised PbTRAP-FLP/EXP2-2A-FRT LS parasites under hyptonic conditions (4% PFA, 0.0075% gluteraldehyde, 0.75× MT-PBS) and co-labelling of KAHRP$_L$-GFP (green) with the PVM marker anti-EXP1 (red). At 20 hpi, KAHRP$_L$-GFP is held in the PV. An average Pearson's coefficient of 0.716 was calculated from 15 cells, indicating a significant degree of co-localisation with EXP1. By 48 hpi LS, the fixation of EXP2-2A causes loss of the KAHRP$_L$-GFP bulges, resulting in GFP localisation throughout the hepatic cytosol. Scale bars 10 μm.

Accumulation of the knob-associated histidine-rich protein conjugated to GFP reporter occurs despite peripheral localisation of EXP2

As the detection of mCherry in Fig. 3B serves as a reporter of the timing of EXP2 expression but does not represent the final localisation of EXP2, we sought to directly confirm whether KAHRP$_L$-GFP was trapped in the PV of LS because EXP2 was absent from the PVM. Here, we fixed HepG2 cells infected with EXP2-HA parasites and probed with anti-HA antibodies and anti-*P. berghei* sera (Fig. 5A). As expected, EXP2-HA localized at the parasite periphery from 18 hpi until the formation of the merosome at 65 hpi, when the HA localized to individual merozoites. This result is consistent with our previous observation that *P. berghei exp2* transcript is present throughout LS development (Matthews *et al.*, 2013), and the PVM localisation of *P. falciparum* EXP2 in humanized mice at 5- and 7-days post-infection (Vaughan *et al.*, 2012). Thus, despite the presence of EXP2 at the PVM throughout LS growth (Fig. 5A) and despite KAHRP$_L$-GFP being translocated into the erythrocyte cytosol during the IDC, KAHRP$_L$-GFP could not be actively translocated across the PVM into the hepatocyte cytosol during LS development.

HSP101 is absent from the parasitophorous vacuole in the liver stages

Analysis of *P. falciparum* infected hepatocytes in mice engrafted with human hepatocytes has shown that the core PTEX component PTEX150 co-localizes with EXP2 at the PVM (Vaughan *et al.*, 2012). Conversely, several attempts to localize HSP101 in wildtype *P. berghei* or parasites expressing PbHSP101-HA in LS using antibodies raised against *P. falciparum* HSP101 could not detect HSP101 at the PVM (not shown). We therefore sought to corroborate whether HSP101 is expressed in LS parasites. We probed fixed HepG2 cells infected with HSP101-HA parasites, or EXP2-HA parasites as a positive control, with either HA or EXP2 antibodies (Fig. 5B). As expected, EXP2 could be detected in HSP101-HA LS parasites, which is consistent with HA antibody yielding a strong PVM signal on EXP2-HA parasites. In contrast, whilst the HA antibody reacted against HSP101-HA parasites at the IDC stage as well as sporozoites and LS merozoites, where it gave punctuate staining (Matthews *et al.*, 2013), the same antibody failed to detect a signal at the PVM in LS parasites, despite significantly longer exposure times (Fig. 5B). As HSP101 is an essential PTEX component in the IDC where it is mandatory for protein export, its absence from the PVM of LS is consistent with a failure of KAHRP$_L$-GFP to be exported during LS development.

Discussion

Whilst previous reports indicate EXP2 is likely to be essential to malaria parasites on the basis that the gene encoding this protein cannot be genetically disrupted, this study provides the first direct evidence with the use of FLP/FRT technology that EXP2 is critical for parasite infectivity in a *P. berghei* mouse model of infection.

In the IDC stages of the infection, EXP2 is initially trafficked to the dense granules and is secreted into the PV during invasion, where it becomes tightly associated with the PVM and forms a constituent of the PTEX complex (Bullen *et al.*, 2012). Because EXP2 initially localizes to the PVM in LS and is also expressed in LS merozoites, EXP2 could also play a role in parasite growth in the pre-erythrocytic stages of infection and/or the transition of parasites from the liver to the blood. Our combined results indicate that EXP2 plays a likely role in both of these stages. Although an intact *exp2* locus could be detected in FLP/EXP2-FRT sporozoites by PCR, the reduction in *exp2* transcript in mouse livers combined with the clear defect in infectivity of the FLP/EXP2-FRT parasites demonstrates that excision has occurred in the bulk of parasites in the liver. Nevertheless, the parasite load detected in the liver indicates that some parasites were capable of liver stage development. However, it should be noted that *exp2* transcript, which is already detectable in oocysts (Matthews *et al.*, 2013), may have already been expressed in the mosquito stages prior to expression of the FLP recombinase under the TRAP and UIS4 promoters, as these have peak activity in mid-gut and salivary gland sporozoites respectively (Rosinski-Chupin *et al.*, 2007). Thus, some of the non-excised transcript we observed in sporozoites may represent transcript generated prior to the excision event, thereby complementing EXP2 expression in the conditional FLP/EXP2-FRT parasites and facilitating normal LS development. The excision event would still lead to a failure to express new EXP2 during the later stages of LS development for delivery to the apical organelles in LS merozoites, which would be consistent with the observed decrease in the establishment of IDC parasites.

We anticipated that the inclusion of a mCherry reporter into our transgenic parasites would help determine the contribution of EXP2 in the liver stages as it would allow us to discriminate which hepatocytes were infected with parasites with an excised *exp2* locus and if there was any consequential effect on protein export. The KAHRP$_L$-GFP reporter was selected to analyse protein export because there has been conflicting evidence as to whether protein translocation into the hepatocyte cytosol actually occurs, although this may be because the LS proteins examined may not represent *bona fide* exported proteins. However, instead of detecting the PEXEL-
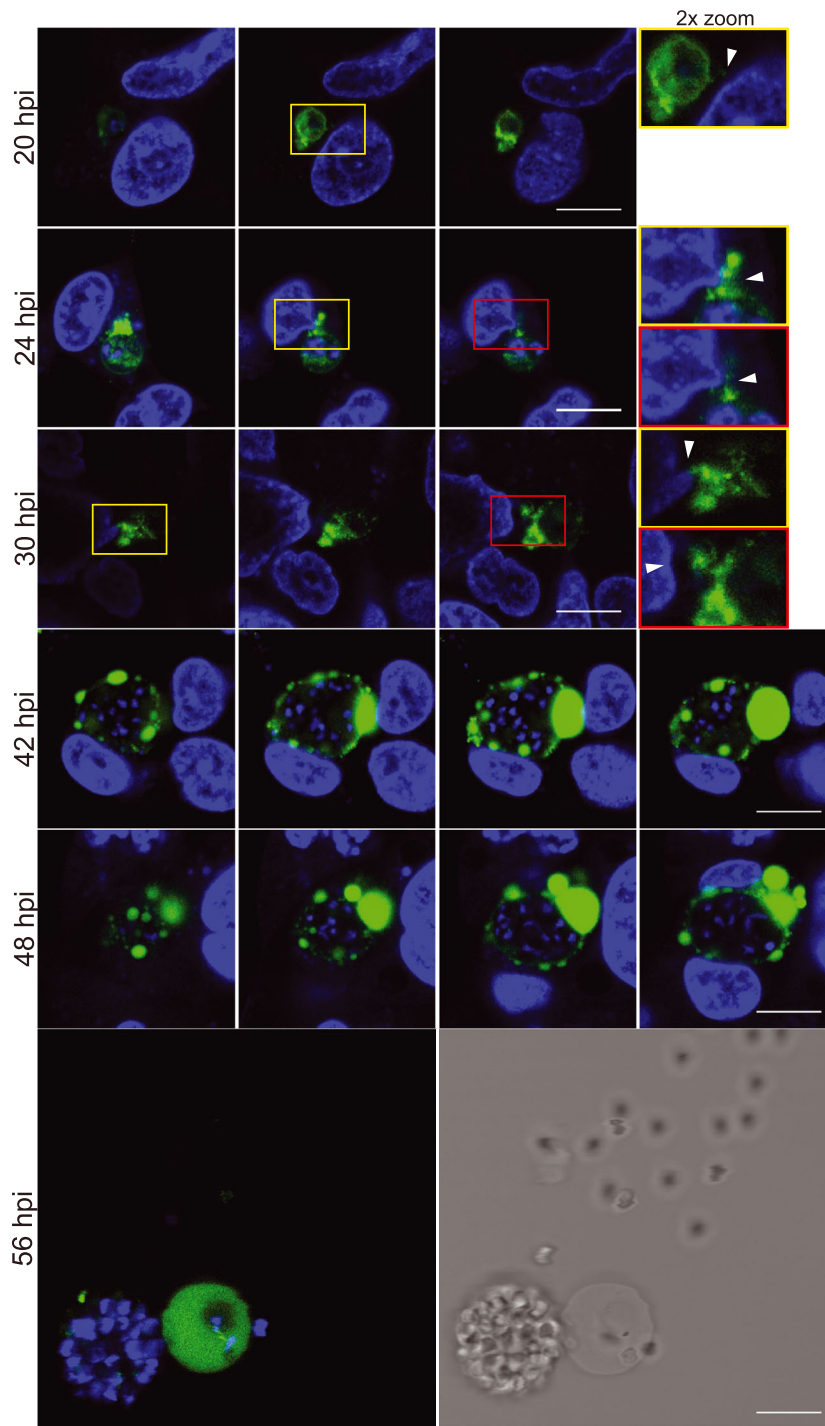
Fig. 4. Optical sections of unfixed, non-excised PbTRAP-FLP/EXP2-2A-FRT infected hepatocytes show that some TVN extensions of 20–30 hpi LS parasites correspond to indentations of the host nucleus (white arrows in the 2× magnification view). The GFP accumulations in the PV form during 42–48 hpi. After merosome formation and PVM degradation, GFP fills the merosome sac prior to the merosome bursting and release of merozoites (from 56 hpi). Scale bars 10 μm.

containing GFP reporter in the hepatocyte cytosol, we observed significant accumulation of GFP in large bulges within the confines of the PVM. The trapping of the GFP in the PVM revealed for the first time that there are regions of the parasite and PVM that are tightly associated, in what appears to be a very similar organisation to the IDC. Although the trapping of the KAHRP$_L$-GFP reporter within the confines of the PVM in the LS does not exclude the possibility that other parasite proteins less tightly folded than GFP are translocated across the PVM (Singh *et al.*, 2007; Orito *et al.*, 2013), our study clearly demonstrated that the active translocation of KAHRP$_L$-GFP into the host cytosol that occurs during the erythrocyte infection did not occur during
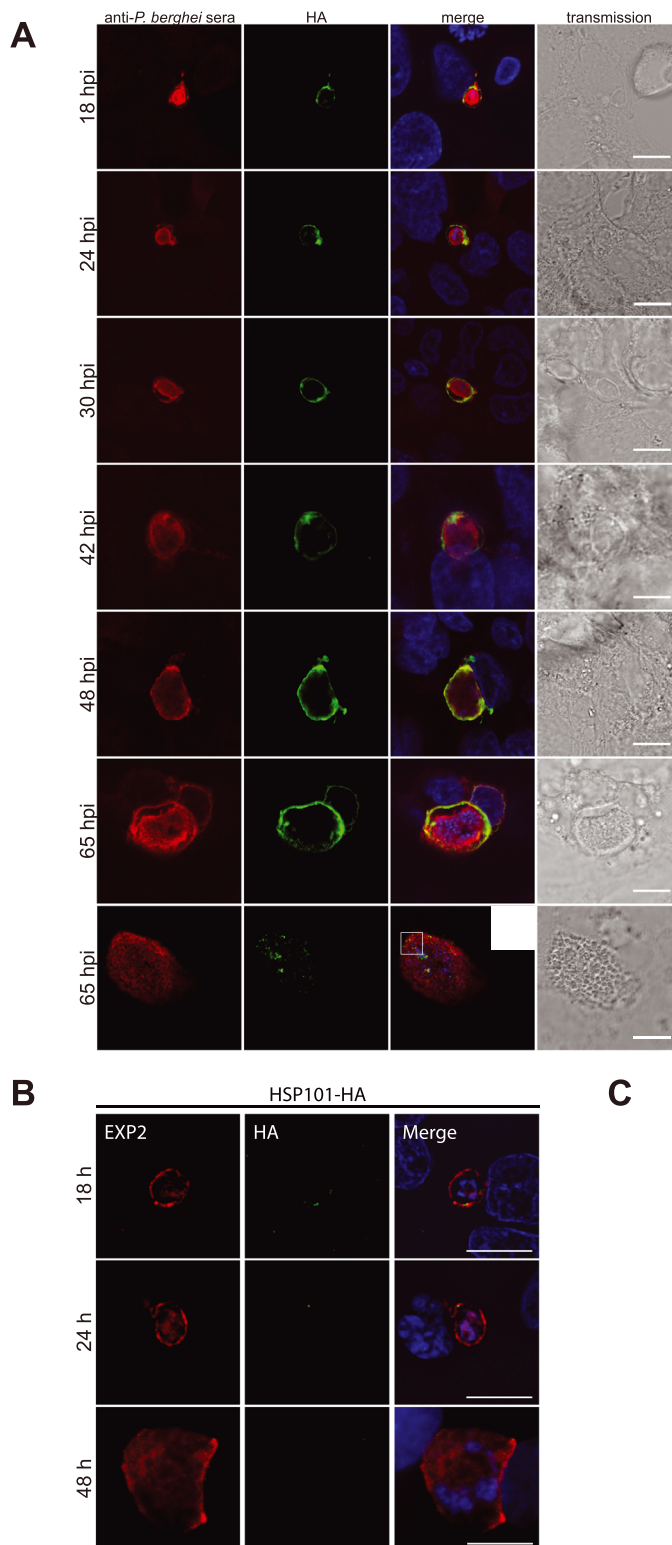
Fig. 5. A. Epifluorescent imaging of EXP2-HA with anti-HA (green) and anti-*P. berghei* hyperimmune serum (red) shows that EXP2 is present and localized to the PVM throughout LS infection, until it is packaged into individual merozoites (2× magnification in inset, bottom panel).
B. Concurrent labelling of HSP101-HA and (**C**) EXP2-HA with anti-HA (green) and anti-EXP2 (red) fails to detect expression of HSP101-HA at the PVM throughout LS development. Exposure times used for detecting anti-HA antibody on HSP101-HA was 2.0 s, significantly longer than that used for EXP2-HA (0.12–0.7 s). Scale bars 10 μm.

hepatic development. This observation is consistent with the localisation of IBIS1, which is also translocated into the erythrocytic cytosol to punctate, Maurer's cleft-like, structures (Ingmundson *et al.*, 2012; Haase *et al.*, 2013)

and its constrained localisation to the parasite PVM and TVN in hepatocytes (Ingmundson *et al.*, 2012; Grutzke *et al.*, 2014). Whilst our KAHRP_L-GFP reporter was secreted outside of the parasite plasma membrane

(Fig. 3B), it could not be detected beyond the extensions of the TVN and PVM, similar to CSP (Cockburn *et al.*, 2011) and a CSP leader-bearing OVA reporter (Montagna *et al.*, 2014). Apart from CSP, LISP2 is the only other parasite protein shown to localize to the hepatocyte cytosol (Orito *et al.*, 2013). However, the final localisation of LISP2 is uncertain, because an mCherry-tagged LISP2 was trapped within the PVM, whilst immunodetection of the protein was localized to the hepatocyte cytosol, possibly due to C-terminal processing of the protein (Orito *et al.*, 2013). The discrepancy in these results may be because fluorescent reporter proteins are not well-secreted by liver stage parasites in general. Thus, identification of more parasite substrates, including PEXEL-negative proteins, is required to confirm if protein translocation into the host cytosol occurs in LS.

The aggregation of KAHRP$_L$-GFP in the PV demonstrates that the PEXEL motif and localisation of EXP2 at the PVM were insufficient for translocation of this reporter into the hepatic host cytosol. In the IDC, the default translocation of KAHRP$_L$-GFP into the erythrocyte cytosol can be blocked in several ways: addition of Brefeldin A inhibits trafficking of KAHRP$_L$-GFP out of the secretory system (Haase *et al.*, 2009), mutations in the PEXEL motif can impair cleavage of the PEXEL by Plasmepsin V (Boddey *et al.*, 2010), deletion of the poly-histidine flank downstream of the PEXEL leads to PV accumulation (Wickham *et al.*, 2001) and additional inhibitory trafficking motifs can override the export signal of KAHRP (Sijwali and Rosenthal, 2010). Additionally, inducible depletion of the essential PTEX components, PTEX150 and HSP101 also trap native cargo in the PV (Beck *et al.*, 2014; Elsworth *et al.*, 2014) as observed here with our KAHRP$_L$-GFP reporter. Our failure to detect the expression of the putative molecular motor of PTEX (HSP101) at the PVM of the pre-erythrocytic stages provides a rationale as to why we could not observe translocation of a GFP reporter across the PVM into the hepatocyte cytosol that can be readily translocated in the IDC. The lack of HSP101 expression is also consistent with a recent report published during this submission that showed the absence of HSP101-mCherry expression during the intrahepatic growth of *P. berghei* (Matz *et al.*, 2015). However, other factors could also be important for protein export, and future studies characterising the expression and localisation of Plasmepsin V, for example, are still warranted. How EXP2 can function independently of HSP101 in the LS demands further examination but requires a more effective conditional strategy than utilized here. EXP2 may, for example, be involved in the uptake of small molecules from the hepatocyte given its ability to complement the function of the GRA17 in *T. gondii*, (Gold *et al.*, 2015) or it may help to insert parasite proteins into the PVM.

Ethics statement

All experiments involving mice were performed in strict accordance with the recommendations of the Australian Government and NHMRC Australian code of practice for the care and use of animals for scientific purposes. Protocols were approved by the Deakin University Animal Welfare Committee (Approval no: AWC G37/2013).

Plasmid construction

The construct pTRAD4-Tet07-EXP2 was generated from pTRAD-Tet07-HSP101 (Elsworth *et al.*, 2014) by replacing the HSP101 5′ UTR that had been inserted into the *Nhe*I and *Bss*HII sites with 0.85 kb of the EXP2 5′ UTR amplified from *P. berghei* ANKA gDNA with DO388 and DO389 (Table S1). The HSP101 CDS that had been inserted into the *Pst*I and *Nhe*I sites was replaced with 1.8 kb of the EXP2 CDS and flanking 3′ UTR sequence amplified with DO387 and TD63. The final construct was sequenced and linearized with *Nhe*I and then transected into *P. berghei* ANKA using standard protocols (Janse *et al.*, 2006).

To enable FLP/FRT conditional knockdown of EXP2 via deletion of its 3′ UTR, the construct pEXP2-FRT was created. To achieve this, the EXP2 3′ UTR was PCR amplified from *P. berghei* gDNA using primers MK73 and MK74, and inserted into the previously described p3′ regFRT vector (Lacroix *et al.*, 2011) at the *Hin*dIII and *Avr*II sites. A partial EXP2 CDS was then amplified with MK71 and MK72 and inserted into the vector at the *Hin*dIII and *Not*I sites, ensuring that the linker region between the EXP2 stop codon and the FRT site was preserved (Lacroix *et al.*, 2011). The final construct comprising the EXP2 CDS and the TRAP 3′ UTR containing FRT sites was sequenced and linearized with *Hin*dIII prior to transfection. To enable conditional FLP/FRT mediated knockdown of EXP2, with an exported KAHRP$_L$-GFP reporter and an mCherry reporter to ascertain expression of EXP2, the following fragments were inserted sequentially into the p3′regFRT vector: (i) the PbHSP70 promoter, amplified with DO241 and DO242 from *P. berghei* and inserted into *Hin*dIII/*Sph*I; (ii) the N-terminal leader of the KAHRP$_L$-GFP, amplified with DO243 and DO244 from pL0035-KAHRP$_L$-GFP (Haase *et al.*, 2013) and inserted into *Xho*I/*Sph*I; (iii) 2A-mCherry, amplified with DO245 and DO246 and inserted into *Sph*I/*Nhe*I; (iv) the *P. berghei* EXP2 3′ UTR, amplified with DO251 and DO252 and inserted into *Mlu*I/*Sac*II; and (v) the *P. berghei* EXP2 CDS, amplified with DO253 and DO254 and inserted into *Sac*II/*Sph*I. The final construct, termed pEXP2-2A-FRT, was sequenced and linearized with *Sac*II prior to transfection. Both pEXP2-FRT and pEXP2-2A-FRT constructs were independently transfected into PbNK65, PbNK65-(UIS4 5′/FLP) and PbNK65-(TRAP 5′/FLP) (Lacroix *et al.*, 2011).

Parasites and drug treatment

All parasites lines used in this study were maintained in BALB/c mice as previously described (Matthews *et al.*, 2013). To determine parasitaemias, thin blood smears obtained from tail bleeds were stained with Giemsa and a minimum of 1000 erythrocytes counted. Transfectants were selected by supplying pyrimethamine in the drinking water of mice at a concentration of $0.07 \, \text{mg} \cdot \text{ml}^{-1}$ For *in vivo* exposure of parasites to ATc, mice were randomized into groups of three for each experiment and then given drinking water containing $0.2 \, \text{mg} \cdot \text{ml}^{-1}$ ATc (Sigma) or vehicle control made in 5% sucrose 24 h prior to infection with 10^7 infected erythrocytes.

Life cycle progression, FLP/FRT excision and patency

The 3′ UTR of EXP2 in both the PbEXP2-FRT and PbEXP2-2A-FRT conditional lines was excised using an established protocol for FLP-mediated excision (Lacroix *et al.*, 2011). Briefly, 150–300 mosquitos (3–5 days after emergence) were fed on blood from donor mice infected with the respective *P. berghei* lines at 1–5% parasitaemia. After 16 days at 21°C, the mosquitos were shifted to 26°C for an additional 7 days. On day 23, salivary glands were dissected from the mosquitos into 100 µl phosphate-buffered saline (PBS) and gently disrupted with a sterile pestle. Isolated sporozoites were counted and used to infect recipient 5 week old C57/Bl6 mice by intravenous injection (5000 sporozoites/mouse), with patency determined by daily examination of Giemsa-stained thin blood smears. Alternatively, sporozoites were used to infect HepG2 cells as per standard protocols (Sturm *et al.*, 2006).

Polymerase chain reaction, quantitative reverse transcriptase polymerase chain reaction, southern and western blotting

Diagnostic PCR to test for correct integration of transfection vectors or excision of EXP2 was performed on gDNA from isolated IDC stages or salivary gland sporozoites using the primers in Table S1. For the PbiEXP2 KD line, Southern blotting was additionally performed to ensure the parasite line was clonal using the *P. berghei* EXP2 5′ UTR as a probe, which had been amplified from *P. berghei* with D0388/DO389. To detect the level of EXP2 knock down at the transcriptional level in the IDC and parasite loads in the liver, qRT-PCR was performed. Here, RNA was extracted using Trisure (Invitrogen), followed by treatment with DNaseI (Invitrogen). Complementary DNA (cDNA) was then made using the Omniscript RT Kit (Qiagen) in accordance with the manufacturer's protocol. *P. berghei* *exp2* (DO506/DO507 or DO508/DO509) and *18S rRNA* (DO629/DO330) or mouse *hprt* (DO631/DO632) transcripts were detected using the indicated oligonucleotide combinations in Table S1. To assess liver load, the expression levels of the target genes were normalized against the *hprt* housekeeping gene, whilst for level of knockdown, *exp2* was normalized against 18S rRNA, and gene expression values were calculated based on the $\Delta\Delta$Ct method. Western blotting was performed using parasites extracted from erythrocytes by lysis wih 0.02% saponin on ice for 15 min, followed by three washing steps with PBS. Blots were labelled with anti-*P. falciparum* EXP2 antibody at 1:500, as previously described (Matthews *et al.*, 2013).

Live-cell microscopy

Epifluorescent images of unfixed erythrocytes and HepG2 cells infected with EXP2-2A-FRT parasites and labelled with Hoechst 33342 (Hoechst) were obtained at the indicated time points post-infection with an Axiovert II fluorescence microscope (Zeiss) using a 40× objective. Optical sections from live infected HepG2 cells, labelled with Hoechst, were obtained with a TCS SP2 confocal microscope (Leica), using a 63× objective and the INUBG2E-ONICS incubator stage with manual *z*-stack adjustment (Tokai Hit).

Fixation and immunofluorescence assays

EXP2-2A-FRT parasites in erythrocytes and isolated salivary gland sporozoites were fixed with 4% paraformaldehyde (PFA) and 0.0075% gluteraldehyde in 0.75× mouse tonicity-PBS for 30 min, prior to a wash in 1× PBS and epifluorescent imaging as described earlier. Coverslips seeded with 2×10^5 HepG2 cells were grown for 18 h and then infected with 15 000–20 000 EXP2-2A-FLP sporozoites per well. At the indicated timepoints, cells were fixed with 4% PFA for 30 min, washed three times in PBS and permeabilized with 0.1% Triton X-100 for 30 min. HepG2 cells infected with EXP2-HA or HSP101-HA (Matthews *et al.*, 2013) were fixed with 4% PFA for 30 min prior to permeabilisation with ice-cold methanol. The fixed and permeabilized infected HepG2 cells were labelled with 4'6-diamidino-2-phenylindole and either anti-*P. berghei* antiserum at 1:250 (Matthews *et al.*, 2013), anti-HA antibodies at 1:500 (Roche), anti-EXP2 at 1:500 or anti-PbEXP1 antiserum at 1:250. Co-localisation analysis was performed using the JACoP plugin in ImageJ (Bolte and Cordelieres, 2006; Schneider *et al.*, 2012).

Statistics

All graphs and data generated in this study were analysed using GraphPad Prism 6.0b Software (MacKiev, Boston, MA, USA). Unpaired *t*-tests using parametric distribution were performed to measure differences between parasite populations, whilst a log-rank (Mantel-Cox) test was performed for patency analysis. A *P* value < 0.05 was considered significant.

Acknowledgements

References

Beck, J.R., Muralidharan, V., Oksman, A., and Goldberg, D.E. (2014) HSP101/PTEX mediates export of diverse malaria effector proteins into the host erythrocyte. *Nature* **511**: 592–595.

Boddey, J.A., and Cowman, A.F. (2013) *Plasmodium* nesting: remaking the erythrocyte from the inside out. *Annu Rev Microbiol* **67**: 243–269.

Boddey, J.A., Hodder, A.N., S,. G., Gilson, P.R., Patsiouras, H., Kapp, E.A., *et al.* (2010) An aspartyl protease directs malaria effector proteins to the host cell. *Nature* **463**: 627–631.

Bolte, S., and Cordelieres, F.P. (2006) A guided tour into subcellular colocalization analysis in light microscopy. *J Microsc* **224**: 213–232.

Bullen, H.E., Charnaud, S.C., Kalanon, M., Riglar, D.T., Dekiwadia, C., Kangwanrangsan, N., *et al.* (2012) Biosynthesis, localisation and macromolecular arrangement of the *Plasmodium falciparum* translocon of exported proteins; PTEX. *J Biol Chem* **287**: 7871–7884.

Cockburn, I.A., Tse, S.W., Radtke, A.J., Srinivasan, P., Chen, Y.C., Sinnis, P., *et al.* (2011) Dendritic cells and hepatocytes use distinct pathways to process protective antigen from *Plasmodium in vivo. PLoS Pathog* **7**: e1001318.

Combe, A., Giovannini, D., Carvalho, T.G., Spath, S., Boisson, B., Loussert, C., *et al.* (2009) Clonal conditional mutagenesis in malaria parasites. *Cell Host Microbe* **5**: 386–396.

de Koning-Ward, T.F., Gilson, P.R., Boddey, J.A., Rug, M., Smith, B.J., Papenfuss, A.T., *et al.* (2009) A newly discovered protein export machine in malaria parasites. *Nature* **459**: 945–949.

Elsworth, B., Matthews, K., Nie, C.Q., Kalanon, M., Charnaud, S.C., Sanders, P.R., *et al.* (2014) PTEX is an essential nexus for protein export in malaria parasites. *Nature* **511**: 587–591.

Giovannini, D., Spath, S., Lacroix, C., Perazzi, A., Bargieri, D., Lagal, V., *et al.* (2011) Independent roles of apical membrane antigen 1 and rhoptry neck proteins during host cell invasion by apicomplexa. *Cell Host Microbe* **10**: 591–602.

Gold, D.A., Kaplan, A.D., Lis, A., Bett, G.C., Rosowski, E.E., Cirelli, K.M., *et al.* (2015) The *Toxoplasma* dense granule proteins GRA17 and GRA23 mediate the movement of small molecules between the host and the parasitophorous vacuole. *Cell Host Microbe* **17**: 642–652.

Grutzke, J., Rindte, K., Goosmann, C., Silvie, O., Rauch, C., Heuer, D., *et al.* (2014) The spatiotemporal dynamics and membranous features of the *Plasmodium* liver stage tubovesicular network. *Traffic* **15**: 362–382.

Haase, S., and de Koning-Ward, T.F. (2010) New insights into protein export in malaria parasites. *Cell Microbiol* **12**: 580–587.

Haase, S., Hanssen, E., Matthews, K., Kalanon, M., and de Koning-Ward, T.F. (2013) The exported protein PbCP1 localises to cleft-like structures in the rodent malaria parasite. *Plasmodium berghei. PLoS One* **8**(4): e61482.

Haase, S., Herrmann, S., Gruring, C., Heiber, A., Jansen, P. W., Langer, C., *et al.* (2009) Sequence requirements for the export of the *Plasmodium falciparum* Maurer's clefts protein REX2. *Mol Microbiol* **71**: 1003–1017.

Hliscs, M., Nahar, C., Frischknecht, F., and Matuschewski, K. (2013) Expression profiling of *Plasmodium berghei* HSP70 genes for generation of bright red fluorescent parasites. *PLoS One* **8**: e72771.

Ingmundson, A., Nahar, C., Brinkmann, V., Lehmann, M.J., and Matuschewski, K. (2012) The exported *Plasmodium berghei* protein IBIS1 delineates membranous structures in infected red blood cells. *Mol Microbiol* **83**: 1229–1243.

Janse, C.J., Ramesar, J., and Waters, A.P. (2006) High-efficiency transfection and drug selection of genetically transformed blood stages of the rodent malaria parasite *Plasmodium berghei. Nat Protoc* **1**: 346–356.

Lacroix, C., Giovannini, D., Combe, A., Bargieri, D.Y., Spath, S., Panchal, D., *et al.* (2011) FLP/FRT-mediated conditional mutagenesis in pre-erythrocytic stages of *Plasmodium berghei. Nat Protoc* **6**: 1412–1428.

Matthews, K., Kalanon, M., Chisholm, S.A., Sturm, A., Goodman, C.D., Dixon, M.W., *et al.* (2013) The *Plasmodium* translocon of exported proteins (PTEX) component thioredoxin-2 is important for maintaining normal blood-stage growth. *Mol Microbiol* **89**: 1167–1186.

Matz, J.M., Goosmann, C., Brinkmann, V., Grutzke, J., Ingmundson, A., Matuschewski, K., *et al.* (2015) The *Plasmodium berghei* translocon of exported proteins reveals spatiotemporal dynamics of tubular extensions. *Sci Rep* **5**: 12532.

Matz, J.M., Matuschewski, K., and Kooij, T.W. (2013) Two putative protein export regulators promote *Plasmodium* blood stage development *in vivo. Mol Biochem Parasitol* **191**: 44–52.

Montagna, G.N., Beigier-Bompadre, M., Becker, M., Kroczek, R.A., Kaufmann, S.H., and Matuschewski, K. (2014) Antigen export during liver infection of the malaria parasite augments protective immunity. *mBio* **5**: e01321–01314.

Orito, Y., Ishino, T., Iwanaga, S., Kaneko, I., Kato, T., Menard, R., *et al.* (2013) Liver-specific protein 2: a *Plasmodium* protein exported to the hepatocyte cytoplasm and required for merozoite formation. *Mol Microbiol* **87**: 66–79.

Schneider, C.A., Rasband, W.S., and Eliceiri, K.W. (2012) NIH image to ImageJ: 25 years of image analysis. *Nat Methods* **9**: 671–675.

Sijwali, P.S., and Rosenthal, P.J. (2010) Functional evaluation of *Plasmodium* export signals in *Plasmodium berghei* suggests multiple modes of protein export. *PLoS One* **5**: e10227.

Singh, A.P., Buscaglia, C.A., Wang, Q., Levay, A., Nussenzweig, D.R., Walker, J.R., *et al.* (2007) *Plasmodium* circumsporozoite protein promotes the development of the liver stages of the parasite. *Cell* **131**: 492–504.

Straimer, J., Lee, M.C., Lee, A.H., Zeitler, B., Williams, A.E., Pearl, J.R., *et al.* (2012) Site-specific genome editing in

Plasmodium falciparum using engineered zinc-finger nucleases. *Nat Methods* **9**: 993–998.

Sturm, A., Amino, R., van de Sand, C., Regen, T., Retzlaff, S., Rennenberg, A., *et al.* (2006) Manipulation of host hepatocytes by the malaria parasite for delivery into liver sinusoids. *Science* **313**: 1287–1290.

Sturm, A., Graewe, S., Franke-Fayard, B., Retzlaff, S., Bolte, S., Roppenser, B., *et al.* (2009) Alteration of the parasite plasma membrane and the parasitophorous vacuole membrane during exo-erythrocytic development of malaria parasites. *Protist* **160**: 51–63.

Tawk, L., Lacroix, C., Gueirard, P., Kent, R., Gorgette, O., Thiberge, S., *et al.* (2013) A key role for *Plasmodium* subtilisin-like SUB1 protease in egress of malaria parasites from host hepatocytes. *J Biol Chem* **288**: 33336–33346.

Tilley, L., McFadden, G., Cowman, A., and Klonis, N. (2007) Illuminating *Plasmodium falciparum*-infected red blood cells. *Trends Parasitol* **23**: 268–277.

Vaughan, A.M., Mikolajczak, S.A., Wilson, E.M., Grompe, M., Kaushansky, A., Camargo, N., *et al.* (2012) Complete *Plasmodium falciparum* liver-stage development in liver-chimeric mice. *J Clin Invest* **122**: 3618–3628.

Wickham, M.E., Rug, M., Ralph, S.A., Klonis, N., McFadden, G.I., Tilley, L., *et al.* (2001) Trafficking and assembly of the cytoadherence complex in *Plasmodium falciparum*-infected human erythrocytes. *EMBO J* **20**: 5636–5649.

Zhang, M., Mishra, S., Sakthivel, R., Rojas, M., Ranjan, R., Sullivan, W.J., Jr., *et al.* (2012) PK4, a eukaryotic initiation factor 2alpha(eIF2alpha) kinase, is essential for the development of the erythrocytic cycle of *Plasmodium*. *Proc Natl Acad Sci U S A* **109**: 3956–3961.

Supporting information

Additional Supporting Information may be found in the online version of this article at the publisher's web-site:

Fig. S1: Confocal images of unfixed hepatocytes infected with EXP2-2A 18 - 20 hpi. KAHRPL-GFP is not translocated across the PVM but instead is trapped in the PV. The GFP localisation delineates the circular form of the parasite and forms elongated clusters and tubules (white arrows). Scale bars 10 mm.

Table S1: Primers for cloning and checking intergration.